Detection of an Ultra Low Velocity Zone beneath Central Mexico with PcP Waveform Modeling

A Senior Project
presented to
the Faculty of the Physics Department
California Polytechnic State University, San Luis Obispo

In Partial Fulfillment
of the Requirements for the Degree
Bachelor of Science

by

David James Buckley

March, 2014

Detection of an Ultra-Low Velocity Zone beneath Central Mexico with *PcP* Waveform Modeling

Abstract

PcP phases from a Guatemalan earthquake recorded at Nevada stations of the International seismic network (IM) display evidence of anomalous seismic structure at the core-mantle boundary (CMB); in particular, pre- and post-cursor phases to *PcP* and *ScP*. The data is examined for evidence of an ultra-low velocity zone (ULVZ) by identifying and modeling precursors to *PcP*. Precursory arrivals to *PcP* may be generated by the interaction of *PcP* with a thin layer above the core-mantle boundary (CMB). One-dimensional modeling demonstrates that standard earth models of the core-mantle boundary, which lack ULVZ structure, cannot produce the observed *PcP* data. An ULVZ model with thickness of 7.5 km, velocity reductions of 10% and 20% for *P* velocity and *S* velocity, respectively, and 20% density increase provides the best fit to the observed *PcP* waveforms. Combining these results with other nearby studies of the CMB region indicate that ultra-low velocity zones are an intermittent and short wavelength feature of the CMB.

Introduction

The core-mantle boundary of the earth occurs at ~2900 km depth and represents a change in composition from dominantly silicate mineralogy in the mantle to the primarily (liquid) iron outer core. An ultra-low velocity zone (ULVZ) is a region above the core-mantle boundary (CMB) with large drops in seismic velocities and changes in density compared to standard earth models (Fig. 1). Proposed explanations for their existence are that they might be regions of partial melt and/or regions of chemical irregularities of the deep mantle by core materials [*Garnero and Vidale*, 1999; *Rost*, 2003]. It has been proposed that ULVZs are potential sources of mantle plumes and may have an effect on the reversals on Earth's magnetic field [*Williams*, 1998; *Garnero and Mcnamara*, 2008].

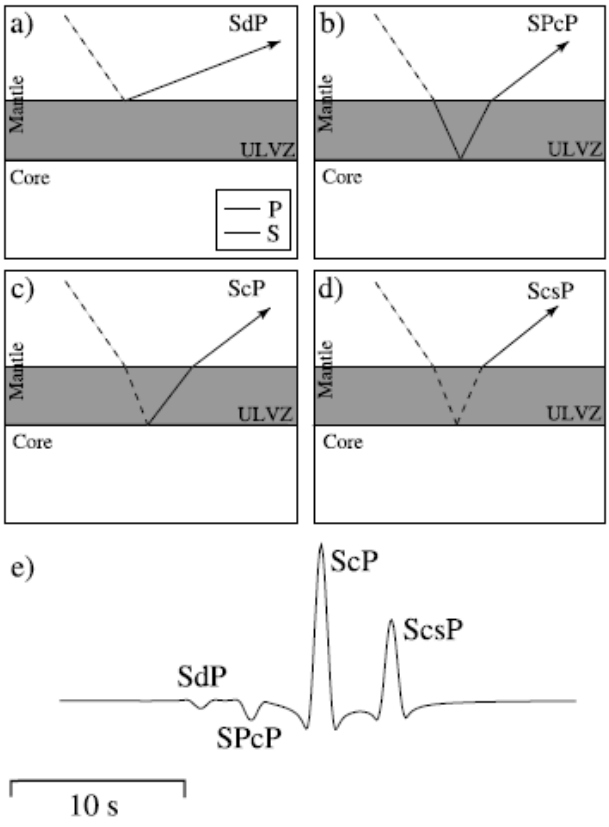

Figure 1. Diagram of pre- and post-cursor phases to *ScP* at the core-mantle boundary. Existence of an ultra-low velocity zone may create both pre- and post-cursors to the main core-mantle boundary reflection. Similar pre- and post-cursors exist for *PcP*. Figure from [*Rost*, 2003].

Numerous studies have been performed to detect evidence of ULVZ structure [*Havens and Revenaugh*, 2001; *Persh et al.*, 2001; *Hutko et al.*, 2009]. Ultra-low velocity zones do not appear as a global feature, or are too thin to detect seismically in most places. For studies where ULVZ's are observed, the ULVZ structures vary widely, with thicknesses ranging from 5 to 50 km, *P* wave velocity reductions up to 15%, and *S* wave velocity reductions of up to 45% [*Rost*, 2003].

The goal of this study is to determine if a ULVZ exists beneath central Mexico at the CMB by modeling stacked *PcP* waveforms recorded at a small aperture array in Nevada. *PcP* waves are *P*-waves which travel to and reflect off the core-mantle boundary, and are recorded back at the surface (Fig. 2). If the core-mantle boundary has no anomalous structure above it, the *PcP* waveform is expected to reflect the initial *P*-wave.

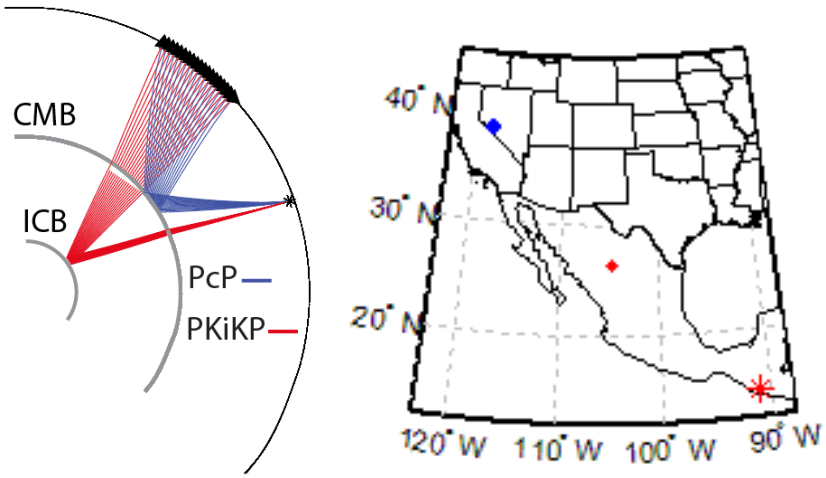

Figure 2. *PcP* and *PKiKP* raypaths and core-mantle boundary sampling. (LEFT) *PcP* and *PKiKP* raypaths are shown from a source to an array of seismometers. *PcP* is the reflection of a *P*-wave off the core-mantle boundary at ~ 2,900 km, and *PKiKP* is the reflection of a *P*-wave off the inner-core boundary at ~ 5,150 km. Note that *PKiKP* passes through the core-mantle boundary twice, and that these regions may be distinct from the core-mantle boundary region from which *PcP* reflects. (RIGHT) Epicenter of Guatemalan earthquake (red star symbol), Nevada seismic stations (blue diamond) and location beneath central Mexico of core-mantle boundary sampled by *PcP*.

Data & Methods

The studied Guatemalan earthquake has an epicenter located at 14.04^0,-91.03^0 and a depth of 112.5 km (http://www.iris.edu/spud/momenttensor/1000975) (Fig. 2). The Nevada stations in the IM network are closely spaced, enabling data stacking to enhance the signal to noise ratio (SNR) of the *PcP* waveform (Fig. 3, 4). A phase-weighted stack was also calculated to examine the coherence of the post-cursor arrivals (Fig. 4) [*Schimmel and Paulssen*, 1997]. The phase-weighted stack suggests that the *PcP* coda is largely incoherent and does not represent significant post-cursory energy of *PcP*. Thus the inability of the one-dimensional modeling presented here to fit the *PcP* coda in the linear stack is not a significant error.

This study exploits the small aperture Nevada array from the IM seismic network (Fig. 3). Linear stacking produces a high SNR waveform (Fig. 4) but the spatial extent of the CMB interrogated is small.

To study the possible CMB structure required to match the observed data, a set of 27 ULVZ models were generated (Table 1) and corresponding synthetic seismograms were generated using the QSEIS software (ftp://ftp.gfz-potsdam.de/pub/home/turk/wang/qseis2006-code+input.zip) [*Wang*, 1999]. QSEIS only allows for one-dimensional modeling of earth structure; thus lateral

and 3-D effects of structure at the CMB on the observed waveforms cannot be captured in the modeling presented here. Preliminary experiments prior to the generation of the suite of ULVZ's in Table 1 determined that a thickness of 7.5 km best fit the phase of the observed stacked *PcP* waveform. Holding thickness constant, we varied V_p, V_s, and ρ (density) in the modeled ULVZ to fit the amplitudes of *PcP*.

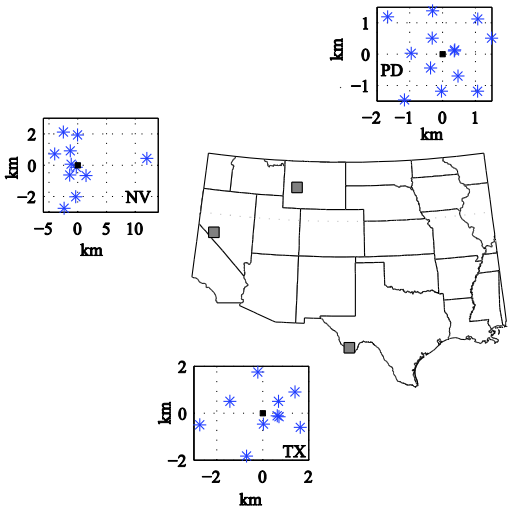

Figure 3. Seismic arrays of the IM network. Nevada (NV), Pinedale, Wyoming (PD), and Texas (TX), stations all recorded the 2007 Guatemalan earthquake. The Nevada IM array is utilized for this study.

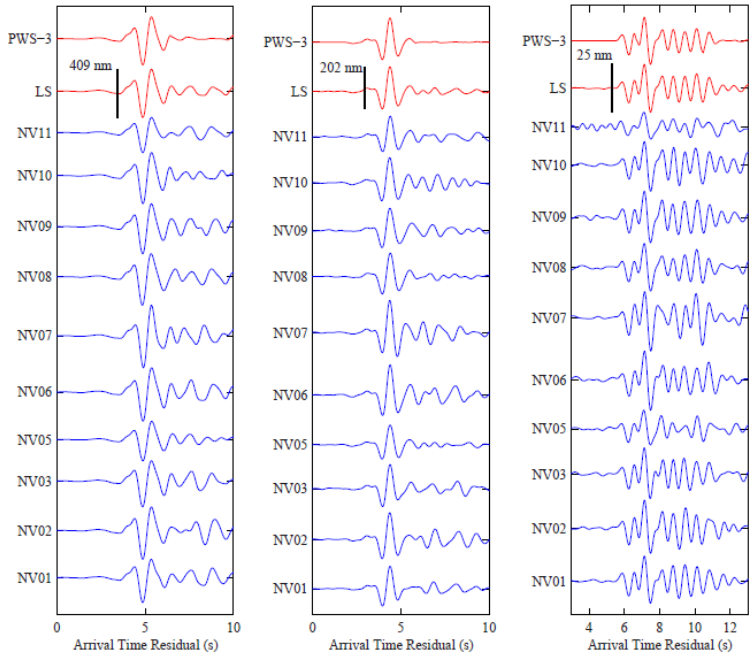

Figure 4. *P*, *PcP*, and *ScP* waveforms recorded at the Nevada array. From left to right: *P*, *PcP*, and *ScP* of the 2007 Guatemalan earthquake. Blue traces are the individual recorded waveforms, LS is a linear stack of the blue waveforms, which were aligned by cross-correlation, and PWS-3 is a phase-weighted stack with exponent 3. The LS is used in the waveform modeling.

Vp (%)	Vs (%)	Density increase (%)	Model #
-5	-10	10	1
-5	-10	20	2
-5	-10	30	3
-5	-20	10	4
-5	-20	20	5
-5	-20	30	6
-5	-30	10	7
-5	-30	20	8
-5	-30	30	9
-10	-10	10	10
-10	-10	20	11
-10	-10	30	12
-10	-20	10	13
-10	-20	20	14
-10	-20	30	15
-10	-30	10	16
-10	-30	20	17
-10	-30	30	18
-15	-10	10	19
-15	-10	20	20
-15	-10	30	21
-15	-20	10	22
-15	-20	20	23
-15	-20	30	24
-15	-30	10	25
-15	-30	20	26
-15	-30	30	27

Table 1. Parameters of ULVZ models. All models were generated for a thickness of 7.5 km. Values are given as a percent change from the PREM earth model (http://www.iris.edu/dms/products/emc-prem/)

Results

From the suite of ULVZ models generated, the best fit model to the waveform (visual fit) was determined to be Model #14: an ULVZ with a thickness of 7.5 km, *P* wave velocity reduction of V_P = -10%, *S* wave velocity reduction of V_S = -20%, and density increase of ρ = +20%. Figure 5 shows the best-fit synthetic seismogram overlaid with the observed waveform. Figure 6 shows the synthetic seismogram for the standard earth model parameters and no ULVZ present. Our fit

matches the initial amplitudes in *PcP* compared to the large amplitude seen in the standard earth model (Fig. 5, 6). The ULVZ models generated do not attempt to fit the *PcP* coda because the phase-weighted stack indicates this in incoherent energy from trace to trace (Fig. 4-6).

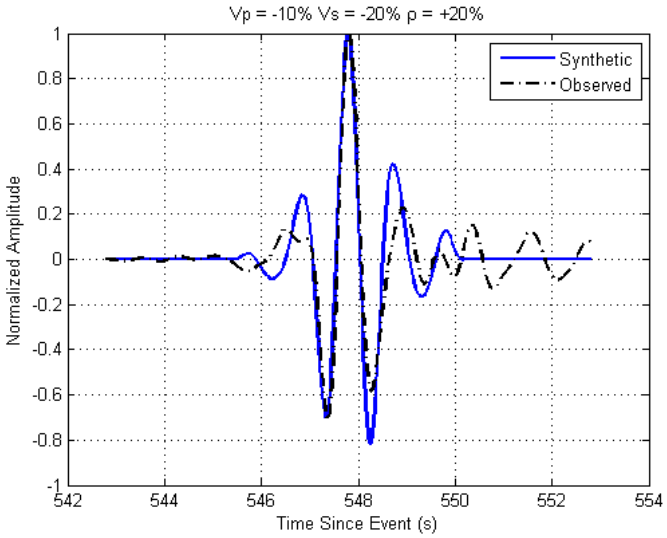

Figure 5. Best-fit ULVZ model overlaid with the observed waveform for *PcP*. The ULVZ parameters used were: thickness of 7.5 km, *P* wave velocity reduction of 10%, *S* wave velocity reduction of 20%, and density increase of 20%.

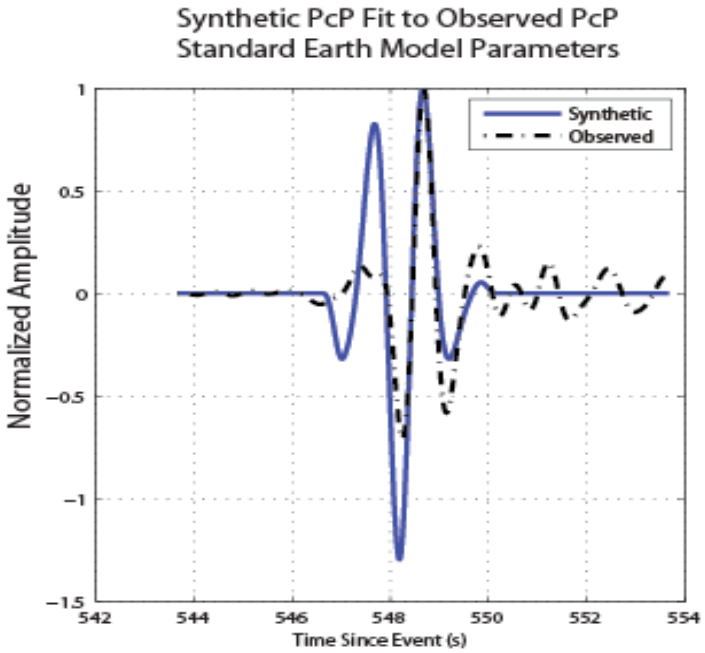

Figure 6. Synthetic seismogram produced using the standard earth model parameters. The lack of any form of ULVZ fails to model the observed waveform's amplitudes accurately.

Discussion

A few previous studies of ULVZ structure at the CMB exist near the region studied here [*Havens and Revenaugh*, 2001; *Persh et al.*, 2001; *Hutko et al.*, 2009]. Evidence for ULVZ structure is varied; while one study finds no evidence for ULVZ structure near the present study area, another study does find ULVZ structure nearby. In aggregate, the present results combined with previous work suggest that ULVZ structure in this region is a short-wavelength feature and thus the processes generating ULVZ are highly spatially variable.

The best fitting model for ULVZ structure presented here suffers from several limitations. First, the modeling of synthetic seismograms is one-dimensional and thus does not account for lateral and 3-D variations in earth structure near the CMB. Second, the considered class of ULVZ models only includes first-order discontinuities and does not consider linear gradients in the ULVZ. Expanding the model space may provide increased fidelity between the synthetic seismograms and the observed data.

It is important to notice that the stacked *PcP* waveform in Figure 4 does not show the precursor to *PcP* as separated from the *PcP* waveform. In contrast, the *ScP* waveform in Figure 4 shows a clear separation between the precursor and the *ScP* reflection. *PcP* and *ScP* sample distinct regions of the core-mantle boundary and so are not expected to have the same features. In the case of *PcP*, the thin ULVZ layer appears to allow for interference between the *PcP* precursor waveform and *PcP* itself, generating a superimposed waveform that is distinct from *PcP*. In particular, the superimposed waveform reduces the initial pulse of the *PcP* waveform that is generated without an ULVZ (Fig. 5, 6). When no ULVZ is present there is a lack of pre-cursory energy to the *PcP* reflection, and the *PcP*-waveform is similar to the *P*-waveform (Fig. 7).

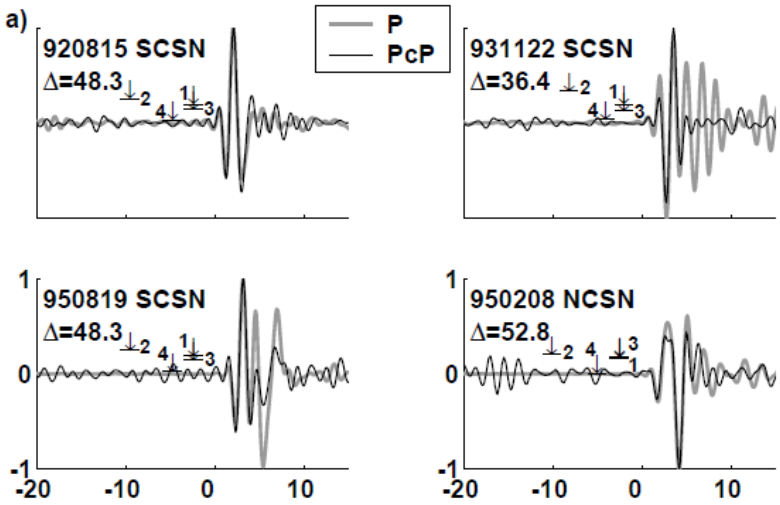

Figure 7. *P* and *PcP* waveforms. *P* and *PcP* waveforms from [*Persh et al.*, 2001] near our sampled location of the CMB. The *P* and *PcP* waveforms are in phase with one another unlike our observed *P* and *PcP* waveforms due to a *PcP* precursor interfering with the main peak.

Understanding CMB structure is important for studies of the core. In particular studies of the inner-core boundary density contrast, which is relatable to the power available for generation of the geomagnetic field, often apply the amplitude ratio of the *PKiKP* phase to the *PcP* phase (Fig. 2) [*Cummins and Johnson*, 1988; *Tkalčić et al.*, 2009]. The *PKiKP/PcP* ratio will be sensitive to the CMB boundary structure and its lateral variations because *PKiKP* travels through the CMB twice, and may sample distinct regions of the CMB compared to *PcP* (Fig. 2). Thus accurately isolating CMB structure in these studies increases the reliability of the *PKiKP/PcP* ratio interpretations for inner-core boundary structure.

The studied Guatemalan earthquake also shows clear precursors to the *ScP* phase (Fig. 4). Future work will apply high-frequency waveform modeling to these waveforms, further constraining the ULVZ structure near the CMB region studied here.

References

Cummins, P., and L. Johnson (1988), Short-period body wave constraints on properties of the Earth's inner core boundary, *J. Geophys. Res. Solid Earth*, *93*(B8), 9058–9074.

Garnero, E. J., and A. K. Mcnamara (2008), Structure and Dynamics of Earth ' s Lower Mantle, *Science*, *320*(May), 626–628.

Garnero, E. J., and J. E. Vidale (1999), ScP; a probe of ultralow velocity zones at the base of the mantle, *Geophys. Res. Lett.*, *26*(3), 377–380.

Havens, E., and J. Revenaugh (2001), A broadband seismic study of the lowermost mantle beneath Mexico: Constraints on ultralow velocity zone elasticity and density, *J. Geophys. Res. Solid Earth*, *106*(B12), 30,809–30,820.

Hutko, A. R., T. Lay, and J. Revenaugh (2009), Localized double-array stacking analysis of PcP: D″ and ULVZ structure beneath the Cocos plate, Mexico, central Pacific, and north Pacific, *Phys. Earth Planet. Inter.*, *173*(1-2), 60–74, doi:10.1016/j.pepi.2008.11.003.

Persh, S. E., J. E. Vidale, and P. S. Earle (2001), Absence of Short-Period ULVZ Precursors to PcP and ScP from two Regions of the CMB, *Geophys. Res. Lett.*, *28*(2), 387–390, doi:10.1029/2000GL011607.

Rost, S. (2003), Small-scale ultralow-velocity zone structure imaged by ScP, *J. Geophys. Res.*, *108*(B1), 2056, doi:10.1029/2001JB001627.

Schimmel, M., and H. Paulssen (1997), Noise reduction and detection of weak, coherent signals through phase weighted stacks, *Geophys. J. Int.*, *130*, 497–505.

Tkalčić, H., B. L. N. Kennett, and V. F. Cormier (2009), On the inner-outer core density contrast from PKiKP/PcP amplitude ratios and uncertainties caused by seismic noise, *Geophys. J. Int.*, *179*(1), 425–443, doi:10.1111/j.1365-246X.2009.04294.x.

Wang, R. (1999), A simple orthonormalization method for stable and efficient computation of Green's functions, *Bull. Seismol. Soc. Am.*, *89*(3), 733–741.

Williams, Q. (1998), A Correlation Between Ultra-Low Basal Velocities in the Mantle and Hot Spots, *Science (80-.).*, *281*(5376), 546–549, doi:10.1126/science.281.5376.546.

Appendix: Modeled and Observed PcP waveforms.

Model #1

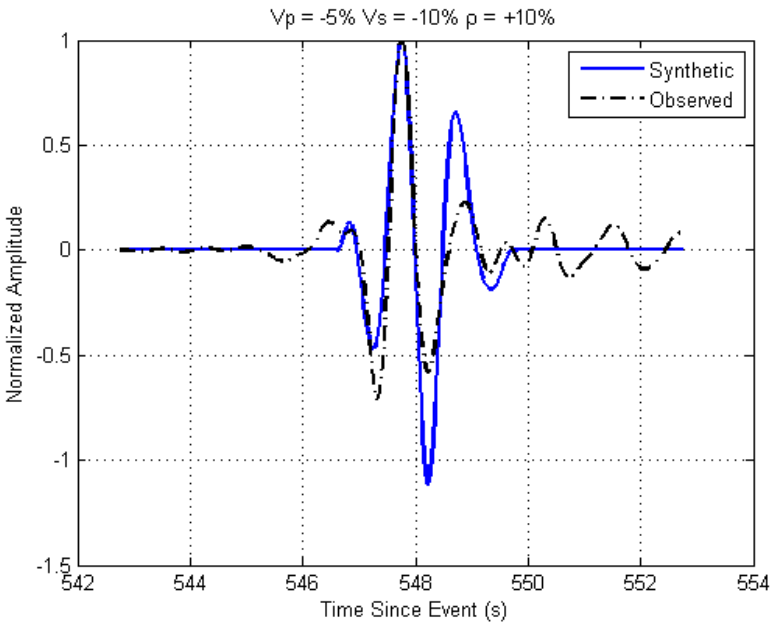

Model #2

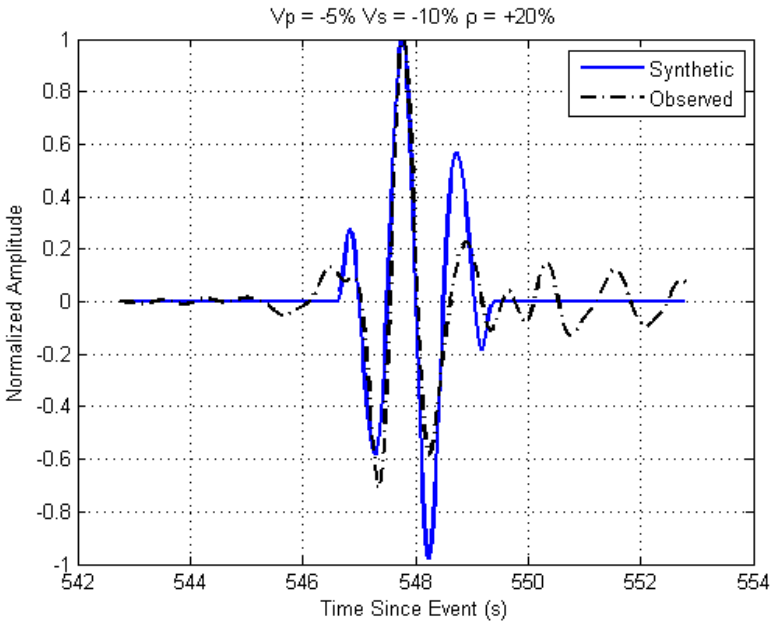

Model #3

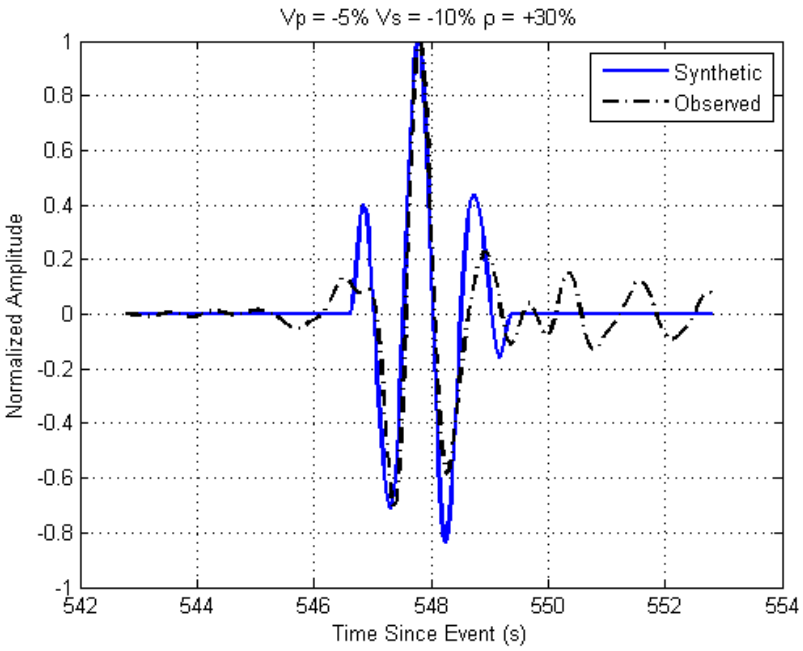

Model #4

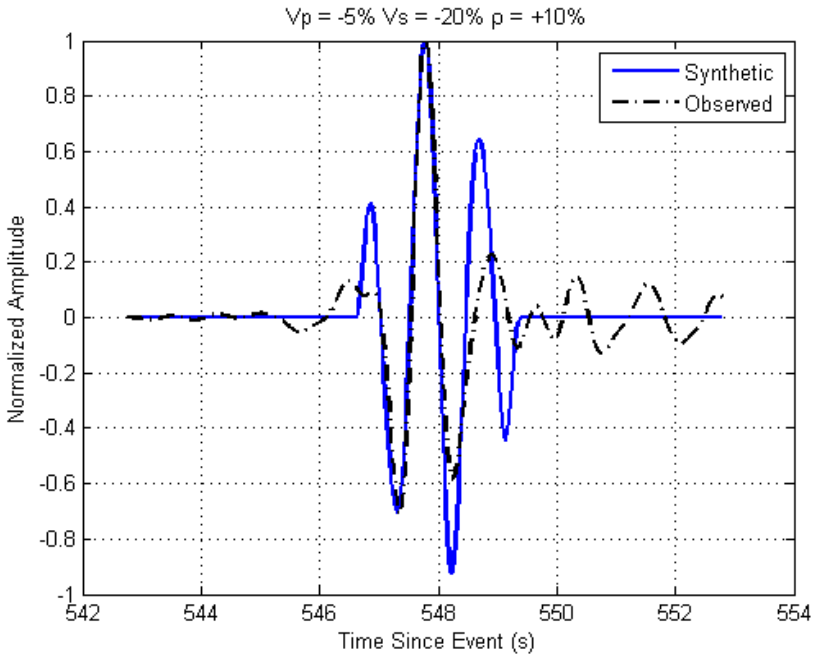

Model #5

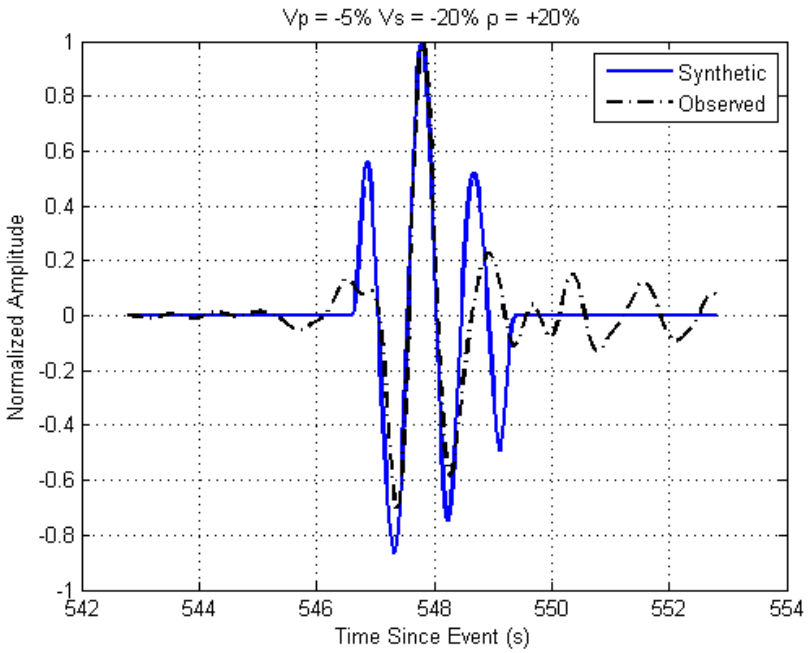

Model #6

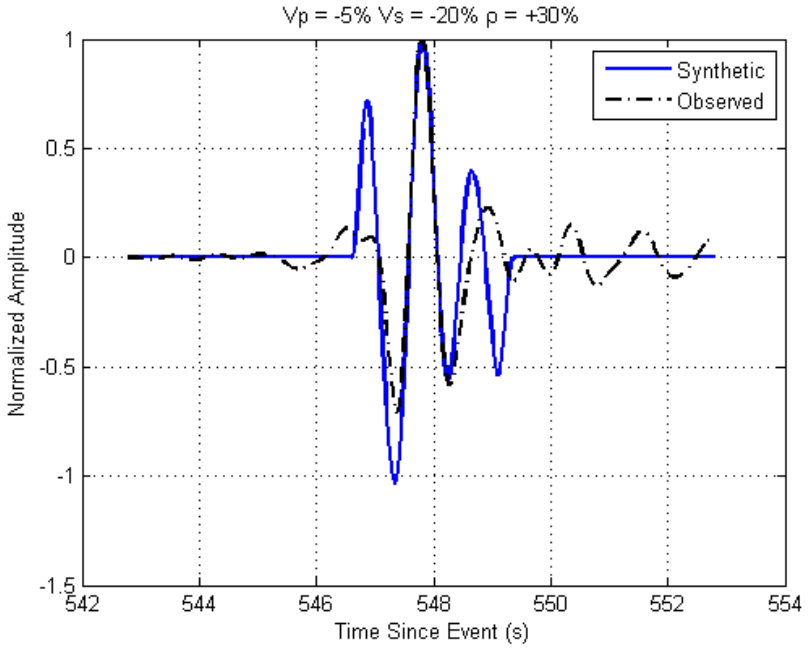

Model #7

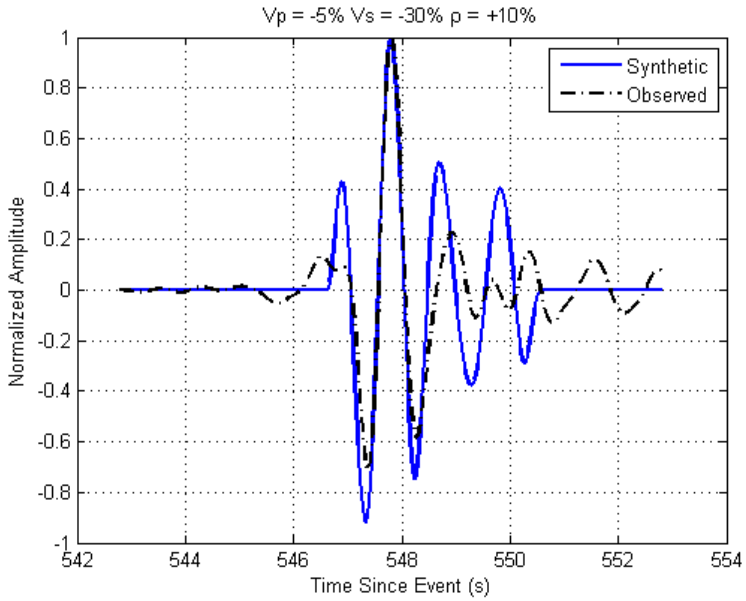

Model #8

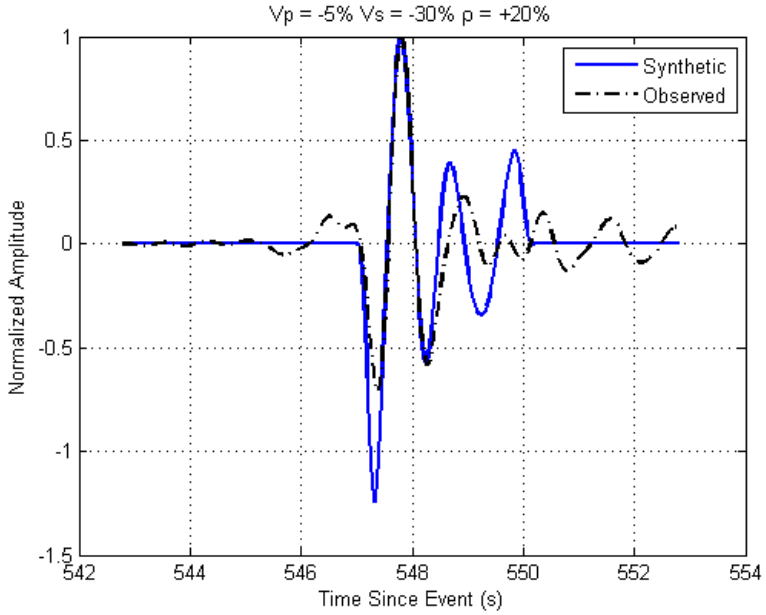

Model #9

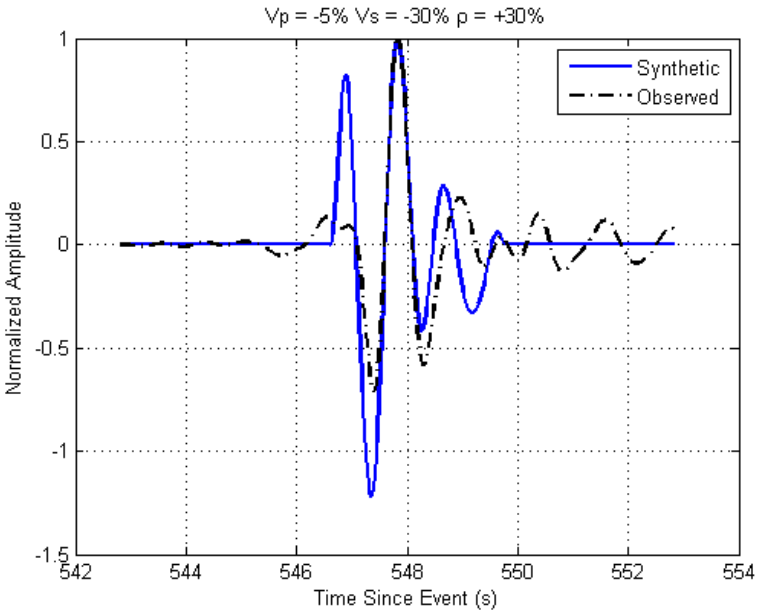

Model #10

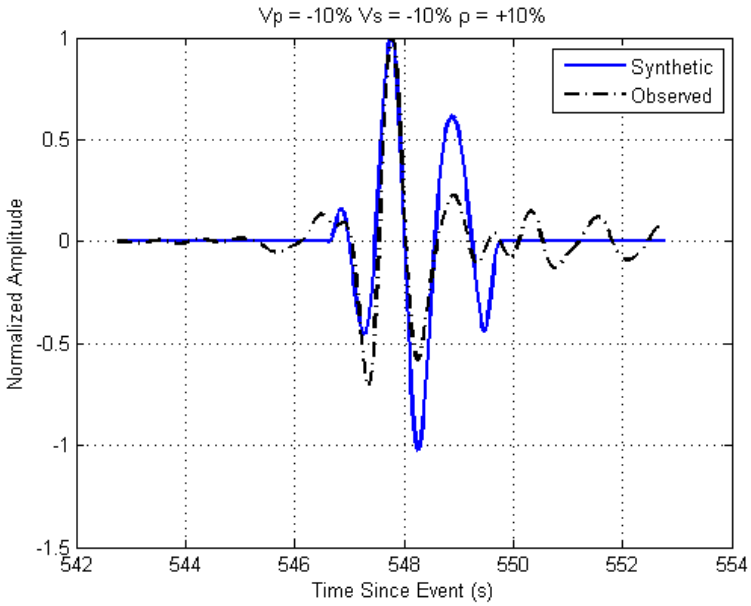

Model #11

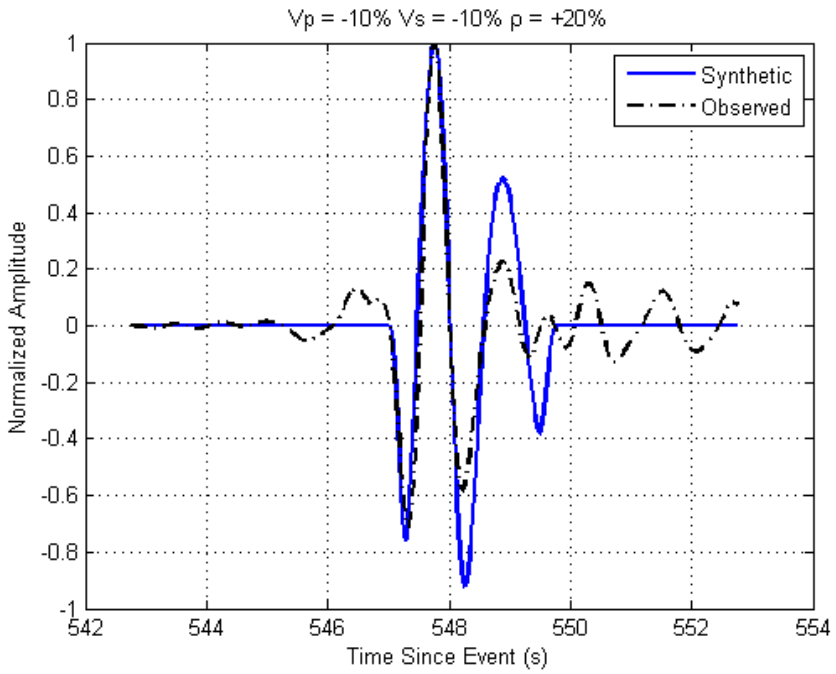

Model #12

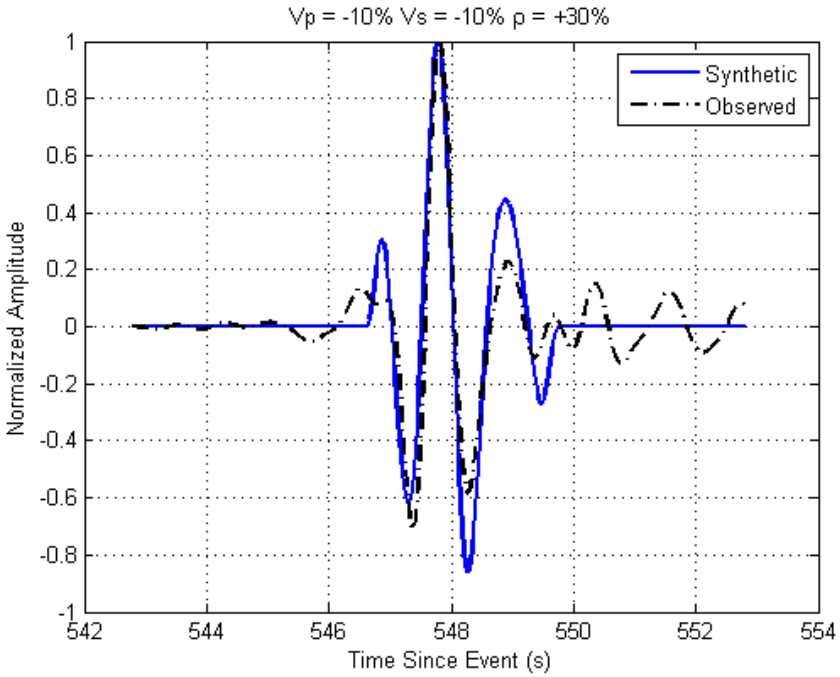

Model #13

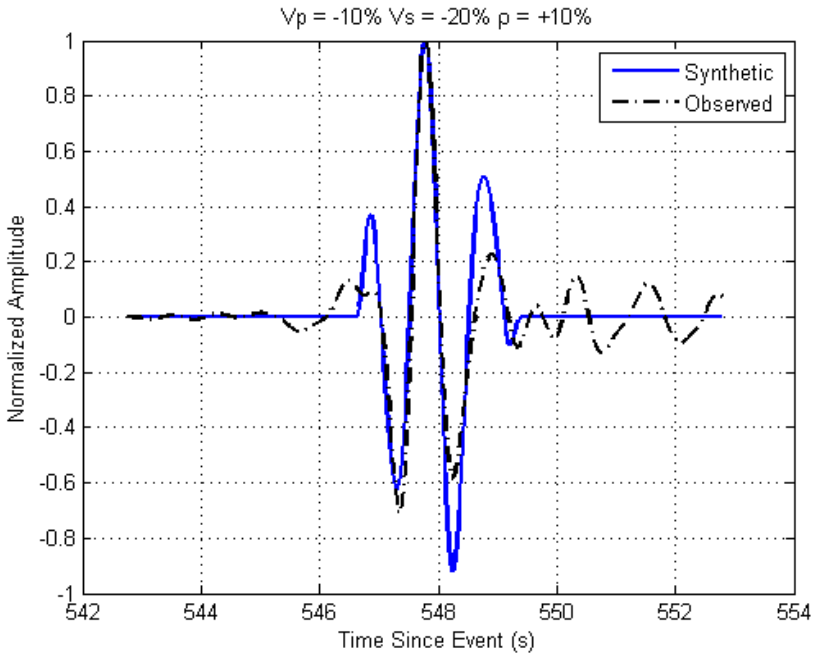

Model #14

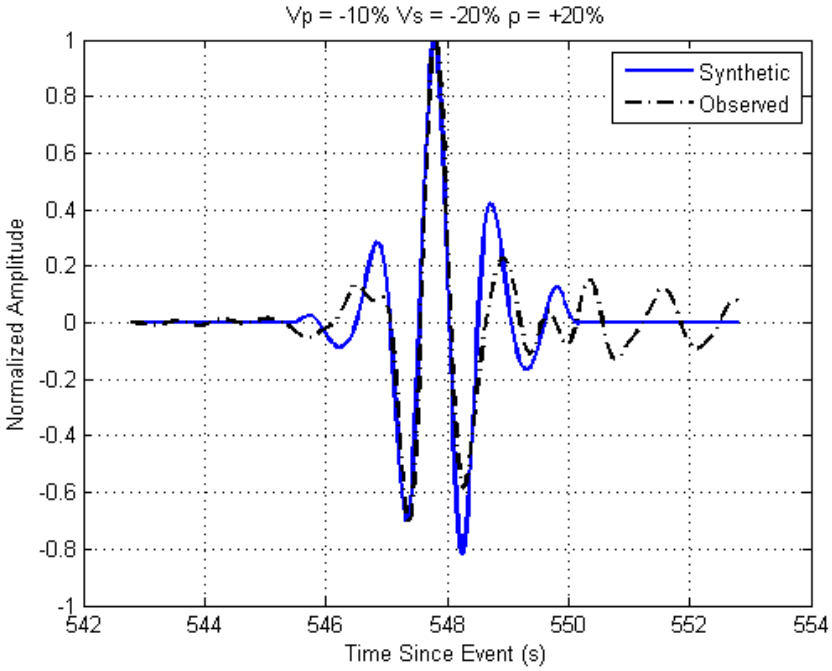

Model #15

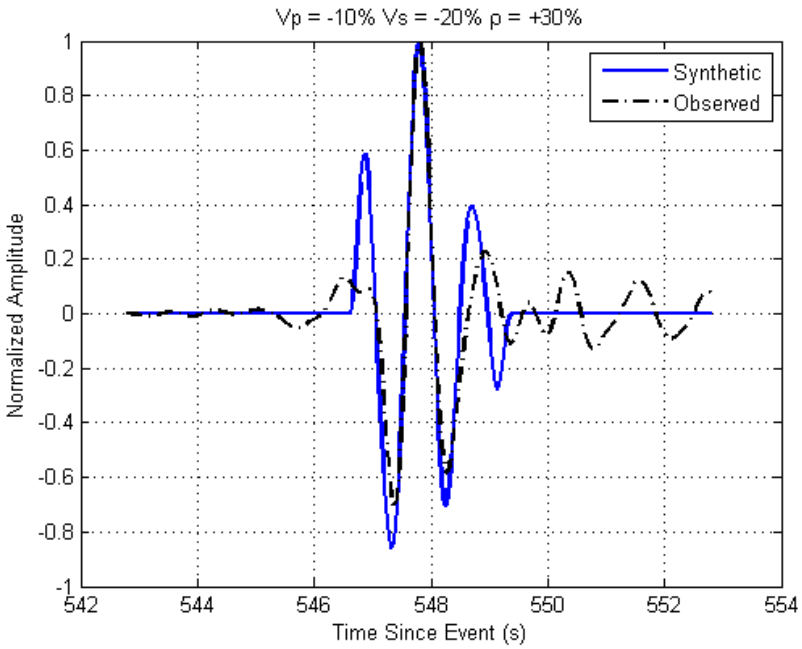

Model #16

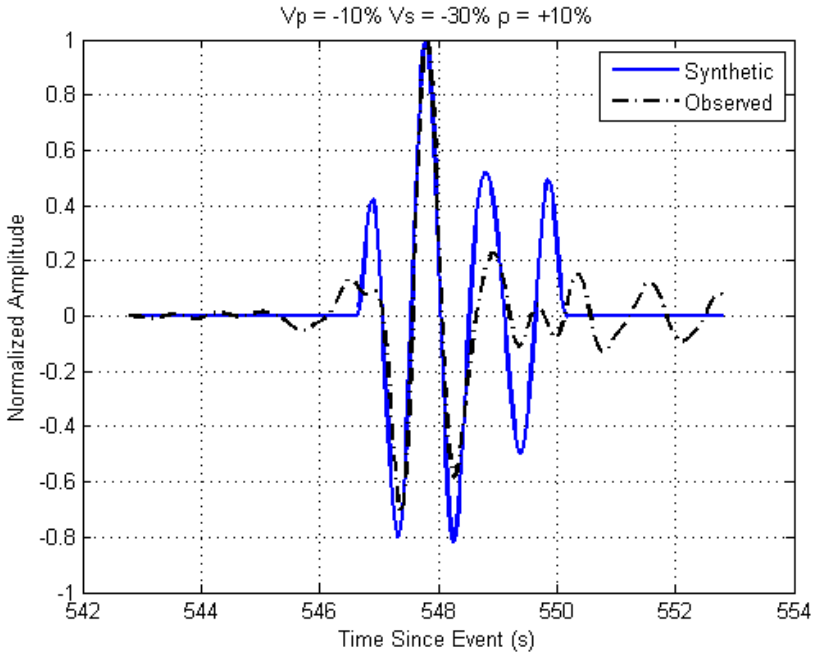

Model #17

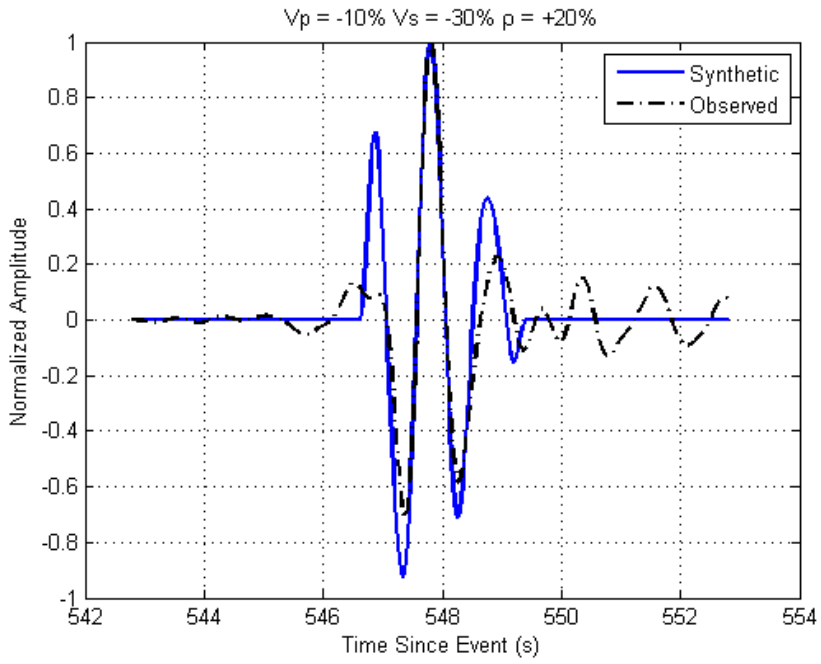

Model #18

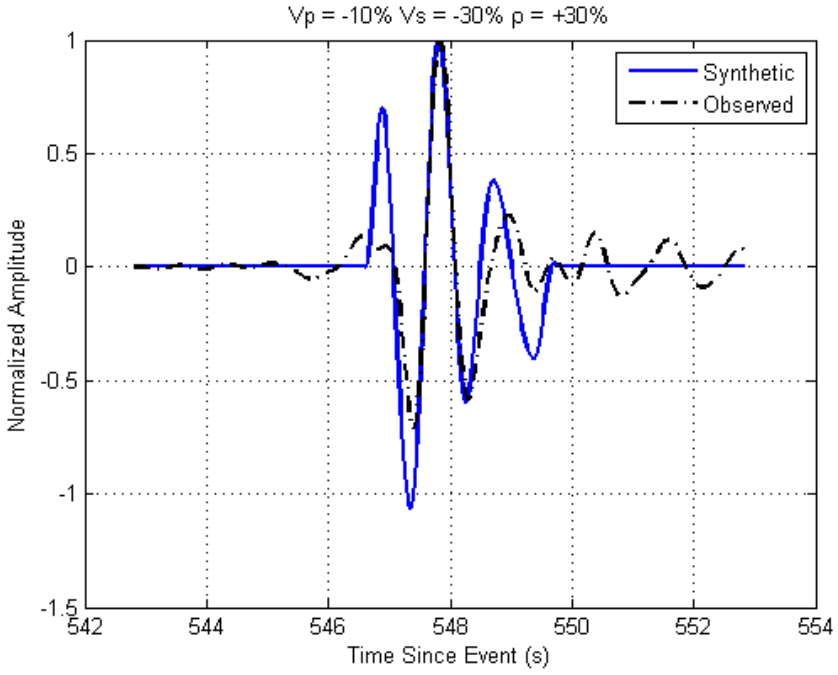

Model #19

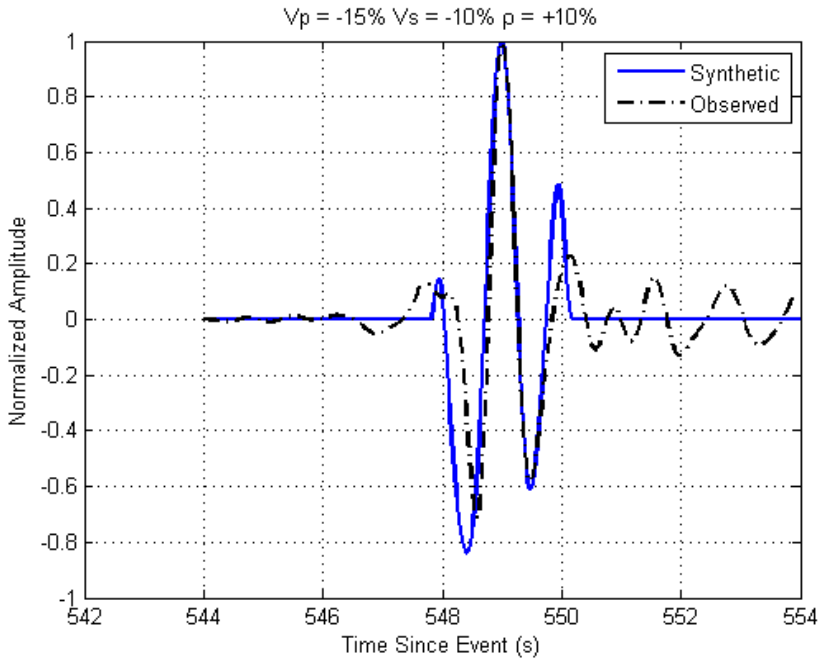

Model #20

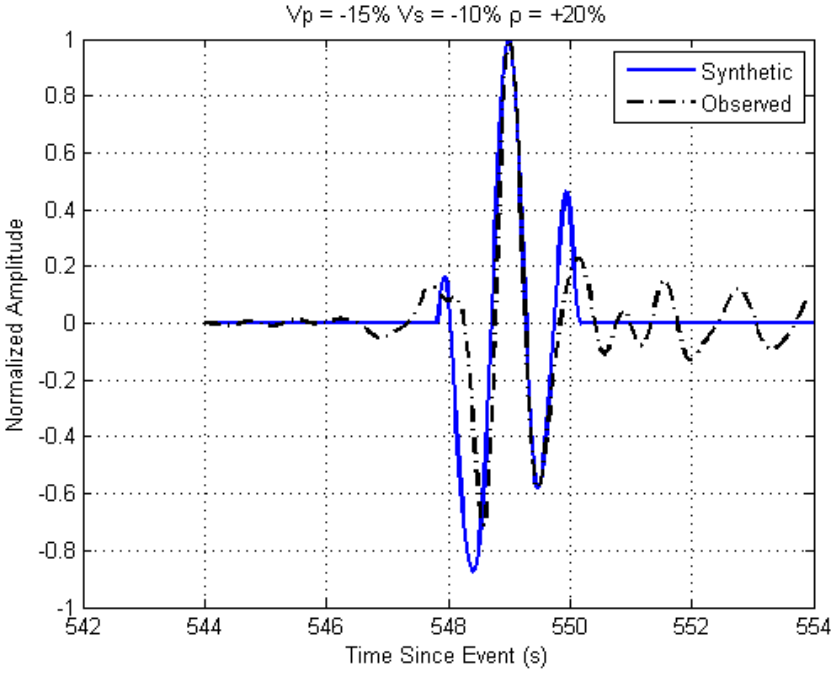

Model #21

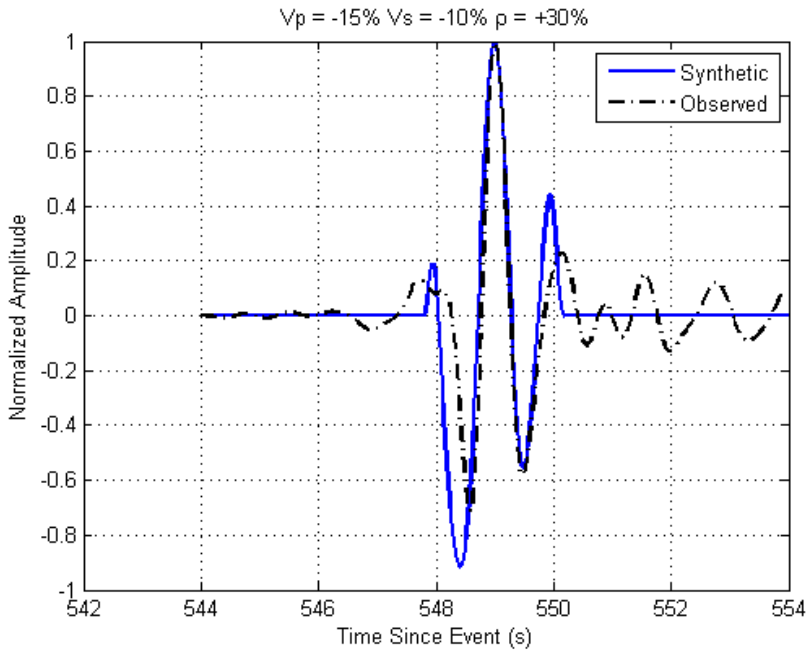

Model #22

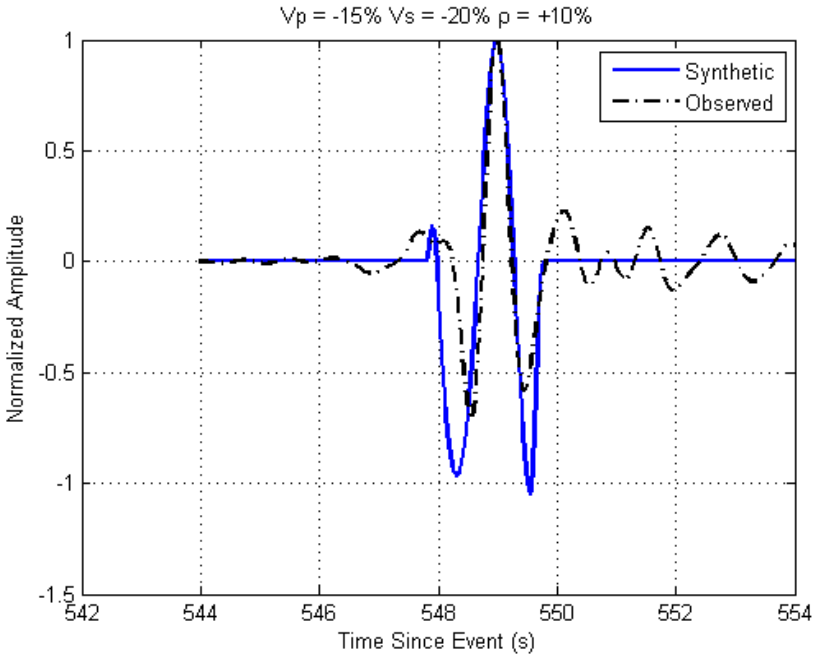

Model #23

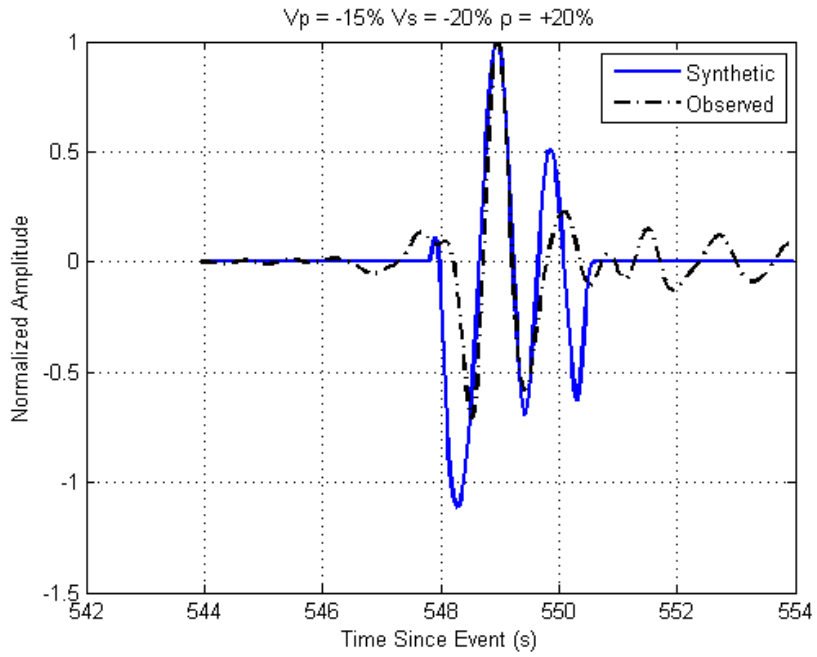

Model #24

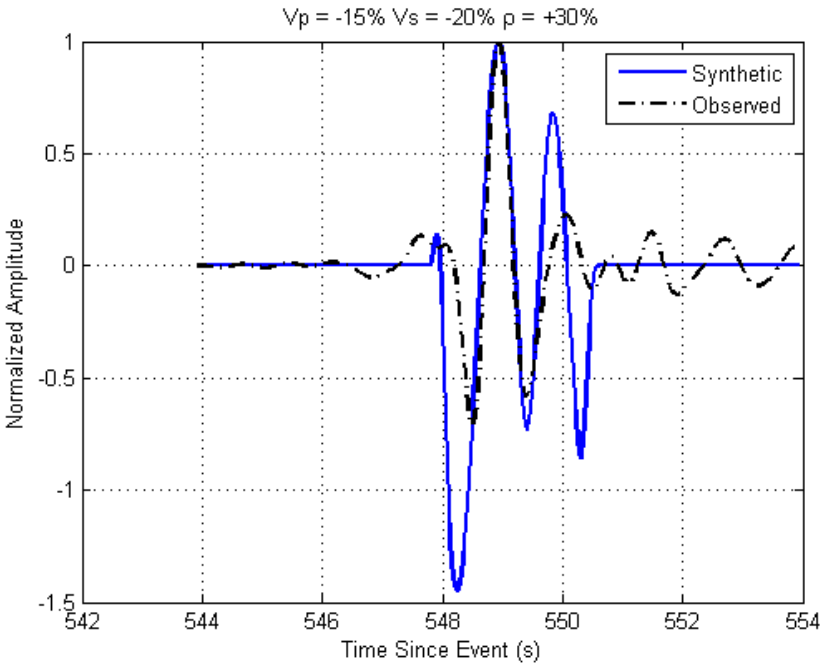

Model #25

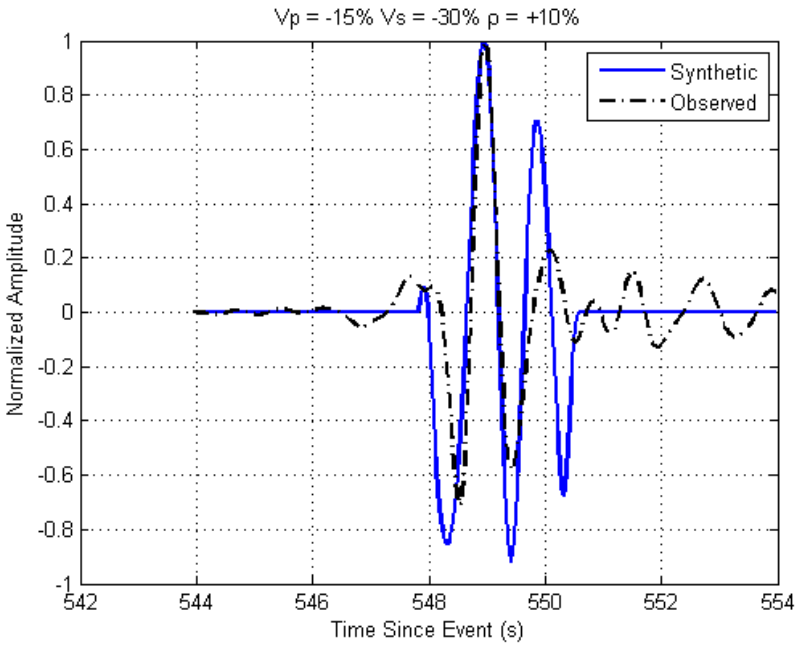

Model #26

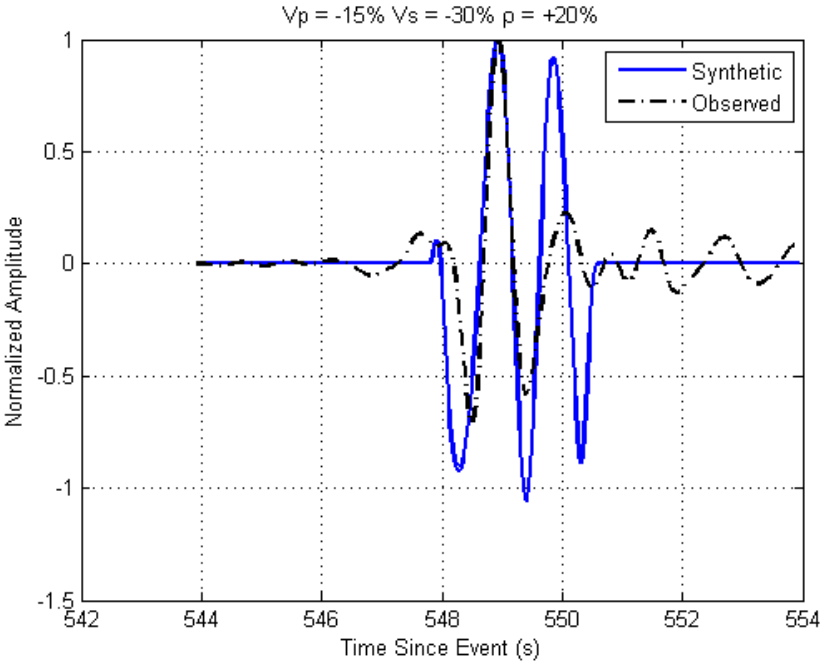

Model #27

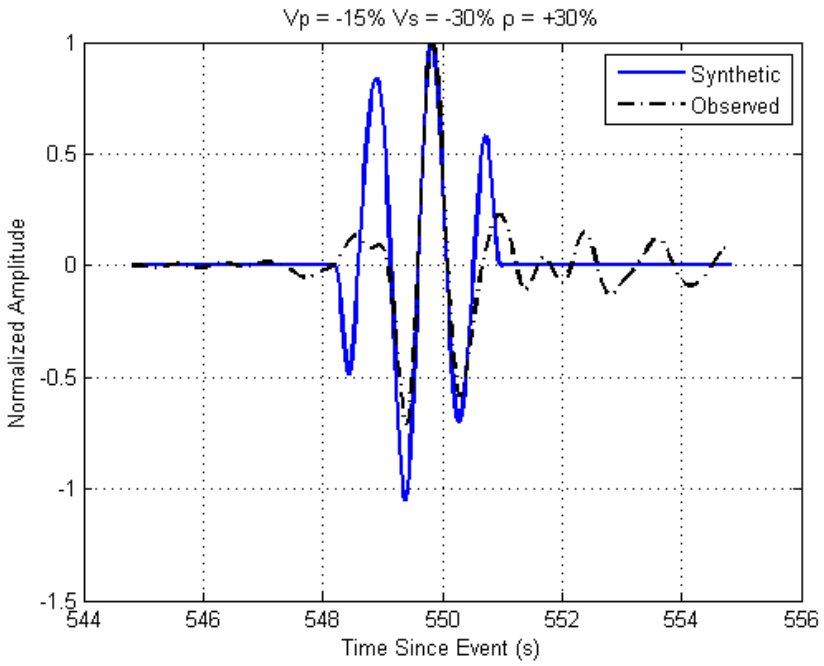
Vp = -15% Vs = -30% ρ = +30%
Synthetic
Observed
Normalized Amplitude
Time Since Event (s)
1
0.5
0
-0.5
-1
-1.5
544
546
548
550
552
554
556